THE JOURNAL OF BIOLOGICAL CHEMISTRY VOL. 289, NO. 33, pp. 23189–23199, August 15, 2014

SLC17A9 Protein Functions as a Lysosomal ATP Transporter and Regulates Cell Viability*

Received for publication, March 21, 2014, and in revised form, June 22, 2014 Published, JBC Papers in Press, June 24, 2014, DOI 10.1074/jbc.M114.567107

Qi Cao‡, Kexin Zhao‡, Xi Zoë Zhong‡, Yuanjie Zou‡, Haichuan Yu‡, Peng Huang‡, Tian-Le Xu§, and Xian-Ping Dong‡1

From the ‡Department of Physiology and Biophysics, Dalhousie University, Halifax B3H 4R2, Nova Scotia, Canada and the §Shanghai Key Laboratory for Tumor Microenvironment and Inflammation, Institute of Medical Sciences, Shanghai Jiao Tong University School of Medicine, Shanghai 200025, China

Background: Lysosomes contain abundant ATP.
Results: SLC17A9 transports ATP into lysosomes. SLC17A9-deficient cells exhibit lysosome dysfunction and undergo subsequent cell death.
Conclusion: SLC17A9 functions as a lysosomal ATP transporter and maintains cell viability.
Significance: This work identifies a molecular mechanism underlying lysosomal ATP accumulation and suggests that ATP functions not only as energy currency but plays a key role in lysosome function.

Lysosomes contain abundant ATP, which is released through lysosomal exocytosis following exposure to various stimuli. However, the molecular mechanisms underlying lysosomal ATP accumulation remain unknown. The vesicular nucleotide transporter, also known as solute carrier family 17 member 9 (SLC17A9), has been shown to function in ATP transport across secretory vesicles/granules membrane in adrenal chromaffin cells, T cells, and pancreatic cells. Here, using mammalian cell lines, we report that SLC17A9 is highly enriched in lysosomes and functions as an ATP transporter in those organelles. SLC17A9 deficiency reduced lysosome ATP accumulation and compromised lysosome function, resulting in cell death. Our data suggest that SLC17A9 activity mediates lysosomal ATP accumulation and plays an important role in lysosomal physiology and cell viability.

The solute carrier (SLC)[2] group of membrane transport proteins includes over 300 members subdivided into 52 families (1, 2). These proteins are located in the plasma membrane and the membranes of intracellular organelles where they transport a variety of solutes across cell membranes. Among these, the SLC17 family mediates activities requiring transmembrane transport of organic anions, including urate secretion (SLC17A1 and SLC17A3), lysosomal export of sialic acid (SLC17A5), and vesicular accumulation of aspartate (SLC17A5) and glutamate (SLC17A5–8). The most recently described family member, SLC17A9, represents a vesicular nucleotide transporter (VNUT) and loads ATP into secretory vesicles in adrenal chromaffin cells (3), T cells (4), and zymogen granules of pancreatic cells (5).

Recent studies indicate that lysosomes store large amounts of ATP (6, 7). However, the molecular mechanisms underlying lysosomal ATP accumulation have not been identified. Because cells contain high (millimolar) levels of ATP in the cytosol, one mechanism could be that lysosomes take up ATP from the cytosol through an ATP transporter located in the lysosomal membrane. Several molecules have been suggested to mediate that activity, including connexins, pannexins, the ATP-binding cassette transporter, maxi-anion channels, and SLC proteins (3, 8, 9). The ATP receptor P2X7 is also implicated in ATP release across the plasma membrane (10). Because SLC17A9 has been shown to transport ATP in intracellular secretory vesicles, we hypothesized that it could also function in lysosomal ATP transport. Here we report that SLC17A9 is highly enriched in lysosomes and actively transports ATP into lysosomes. Compromised SLC17A9 function impaired lysosomal function, subsequently causing lysosomal storage and cell death. Our data suggest a molecular mechanism for lysosomal ATP accumulation and a role for lysosomal ATP in cell viability.

EXPERIMENTAL PROCEDURES

Cell Culture and Transfection—COS1, HEK293T, and C2C12 cells were obtained from the ATCC and maintained in DMEM:nutrient mixture F-12 (F12) supplemented with 10% fetal bovine serum (Invitrogen). Cells were cultured at 37 °C in a 5% CO_2 atmosphere. For some experiments, cells were seeded on 0.01% poly-lysine-coated coverslips and cultured 24 h before further experiments. COS1 and HEK293T cells were transfected using Lipofectamine 2000. C2C12 cells were transfected by electroporation with the Neon® transfection system (Invitrogen) following the optimized protocol of the manufacturer (1650 V, 30 ms, 3 pulses). An ~80% transfection efficiency was achieved regularly.

* This work was supported by start-up funds from the Department of Physiology and Biophysics, Dalhousie University (to X. D.), by a Dalhousie Medical Research Foundation (DMRF) equipment grant, by a DMRF new investigator award, by Canadian Institutes of Health Research (CIHR) Grant MOP-119349, by CIHR New Investigator Award 201109MSH-261462-208625, by Nova Scotia Health Research Foundation Establishment Grant MED-PRO-2011-7485, and by Canada Foundation for Innovation Leaders Opportunity Fund Funding for Research Infrastructure Grant 29291.
[1] To whom correspondence should be addressed: Dept. of Physiology and Biophysics, Dalhousie University, Sir Charles Tupper Medical Bldg., 5850 College St., Halifax NS B3H 4R2, Canada. Tel.: 902-494-3370; Fax: 902-494-1685; E-mail: xpdong@dal.ca.
[2] The abbreviations used are: SLC, solute carrier; VNUT, vesicular nucleotide transporter; GPN, glycyl-phenylalanine 2-naphthylamide; CBX, carbenoxolone; NFA, niflumic acid; DIDS, 4,4′-diisothiocyanostilbene-2,2′-disulfonic acid; PI, propidium iodide.

Antibodies and Reagents—The following primary antibodies were used for immunofluorescence staining and Western blotting: anti-SLC17A9 (MBL Co., Ltd., Nagoya, Japan), anti-Lamp1 (1D4B and H4A3, Developmental Studies Hybridoma Bank), anti-annexin V (Abcam), anti-GM130 (Abcam), anti-EEA1 (Abcam), anti-complex II (Invitrogen), and anti-GAPDH (Santa Cruz Biotechnology). HRP-conjugated secondary antibodies were purchased from Santa Cruz Biotechnology. Alexa Fluor 594 goat anti-rabbit antibody, Alexa Fluor 488 goat anti-rat antibody, fluorescein goat anti-mouse antibody, and Texas Red goat anti-mouse antibody were from Invitrogen.

LysoTracker DND-99 Red (Invitrogen, 50 nM) and Texas Red 10 kDa Dextran (Invitrogen, 1 mg/ml) were used to label lysosomes. DQ-BSA (Invitrogen, 10 μg/ml) was used to assess lysosome function. The following chemicals were also used: GPN (200 μM, Santa Cruz Biotechnology), carbenoxolone (CBX, 20 μM, Sigma), niflumic acid (NFA, 20 μM, Tocris Bioscience), 4,4′-diisothiocyanostilbene-2,2′-disulfonic acid (DIDS, 5 or 20 μM, Tocris Bioscience), and Evans blue (20 μM, Sigma).

Immunocytochemistry—Cells grown on coverslips were washed with PBS twice and fixed in 4% paraformaldehyde in PBS for 15 min at room temperature. Fixed cells were permeabilized with 0.1% Triton X-100 in PBS for 5 min and then blocked with 3% BSA in PBS for 60 min at room temperature. After three PBS washes, cells were incubated with primary antibodies at 4 °C overnight. After three more PBS washes, cells were incubated with fluorescence-conjugated secondary antibodies for 45 min at room temperature in the dark. Images were acquired using a confocal microscope (LSM510, Zeiss) with a ×63 oil immersion objective lens and captured using ZEN2009 software (Zeiss).

Confocal Microscopy—Confocal fluorescent images were taken using an inverted Zeiss LSM510 confocal microscope with ×10 plain or ×63 oil immersion objectives. Sequential excitation wavelengths at 488 nm and 543 nm were provided by argon and helium-neon gas lasers, respectively. BP500–550 and LP560 emission filters were used to collect green and red images in channels 1 and 2, respectively, and then images of the same cell were saved and analyzed with ZEN software. Here the term colocalization refers to the coincident detection of an above-background green and red fluorescent signal. Image size was set at 1024 × 1024 pixels.

RNA Isolation and Plasmid Constructs—Total RNA was isolated from cells harvested in TRIzol reagent (Invitrogen) according to the instructions of the manufacturer. RNA was reverse-transcribed to cDNA using the Moloney Murine Leukemia Virus reverse transcriptional system (Invitrogen). Sequences encoding SLC17A9 were PCR-amplified by *Pfu* DNA polymerase (Agilent) from cDNA derived from C2C12 cells and cloned into the pEGFP-N1 vector (Invitrogen). Primers used were SLC17A9 forward (5′-TGCTCGAGCCATGCCATCCCAGCGCTC-3′) and SLC17A9 reverse (5′-GTGGATCCTCGAG GTCCTCATGAG-TGG-3′). For knockdown studies, we constructed the plasmid pSUPER-SLC17A9. To do so, the pSUPER plasmid (Ambion, Austin, TX) was linearized using BglII and HindIII to facilitate directional cloning. The sequences for mouse SLC17A9-shRNA were as follows: #1, 5′-GATCCCCCCTTCCTGACATTCTCTCGAA-TTCAAGAGATTCGAGAGAATGTCAGGAAGGTTTTTA-3′; #2, 5′-AGCTTAAAAACCTTCCTGACATTCTCTCGAAT-CTCTTGAATTCGAGAGAATGTCAGGAAGGGGG-3′.

Lysosome Isolation by Subcellular Fractionation—Lysosomes were isolated as described previously (30, 31). Briefly, cell lysates were obtained by Dounce homogenization in a homogenizing buffer (0.25 M sucrose, 1 mM EDTA, 10 mM HEPES (pH 7.0)) and then centrifuged at 1500 × *g* (4200 rpm) (Fisher, ST-16R, F15 rotor) at 4 °C for 10 min to remove nuclei and intact cells. Postnuclear supernatants were then fractionated on a Percoll density gradient using a Beckman Optima L-90K ultracentrifuge. For that analysis, the ultracentrifuge tube was layered with 2.5 M sucrose (bottom), 18% Percoll in homogenizing buffer (middle), and sample (top). Samples were centrifuged at 90,000 × *g* (31,300 rpm) at 4 °C for 1 h using a Beckman Coulter 70.1 Ti rotor to obtain light, medium, and heavy membrane fractions. Heavy membrane fractions containing cellular organelles were further layered over a discontinuous iodixanol (v/v; 27, 22.5, 19, 16, 12, and 8%) gradient generated by mixing iodixanol in homogenizing buffer with 2.5 M glucose. The osmolarity of all solutions was 300 mosmol. After centrifugation at 4 °C for 2.5 h at 180,000 × *g* (44,200 rpm), the sample was divided into 12 fractions (0.5 ml each) for further analyses. The biological properties and ionic composition of lysosomes were largely maintained during this procedure because of slowed transport across lysosomal membranes occurring at 4 °C.

Western Blotting—Proteins were analyzed using standard methods. Proteins derived from whole cells or lysosome lysates were resolved on 10% SDS-PAGE. Proteins were then transferred onto PVDF membranes using a semidry transfer apparatus (Bio-Rad). Nonspecific binding was blocked using 5% skim milk in TBS-T (0.1% Tween 20 in 1× Tris-buffered saline (pH 7.4)) for 2 h at room temperature. Membranes were then incubated with specific primary antibody solution at 4 °C overnight with gentle constant shaking. After three thorough TBS-T washes, the membranes were incubated with corresponding HRP-conjugated second antibody at room temperature for 1 h. Immunoreactive bands were visualized using Clear ECL (Bio-Rad) and autoradiography.

Staining for ATP—Cells were pretreated with various transporter inhibitors (CBX, 20 μM; NFA, 20 μM; DIDS or Evans Blue, 5 μM or 20 μM, respectively) for 3 h and then incubated with quinacrine (5 μM) together with LysoTracker Red DND-99 (50 nM) for 30 min at 37 °C and chased for 1 h. Images were acquired using a confocal microscope (Zeiss) with a ×63 oil immersion objective and then collected and analyzed using ZEN2009 (Zeiss). A low laser power (< 0.5%) was used to minimize fluorescence bleaching.

Bioluminescence Measurement of ATP and ATP Uptake Assay—The ATP content of the culture medium or buffer containing freshly isolated lysosomes was measured in triplicate with a microplate luminometer (Fluoroskan Ascent FL microplate fluorometer and luminometer, Thermo Scientific) using the adenosine 5′-triphosphate bioluminescent assay kit (FLAA, Sigma) according to the instructions of the manufacturer. A standard curve was established for each measurement. Samples were adjusted to pH 7.8 to establish conditions optimal to detect ATP. All samples were kept on ice before measurement. Briefly, 100 μl of the ATP assay mix solution was added to the

assay tube and allowed to stand at room temperature for 3 min to hydrolyze endogenous ATP. Then, 100 μl of the sample was added rapidly, mixed gently, and then the plate was read immediately using a luminometer. Blank medium or buffer samples were read in parallel as background, which was subtracted from sample readings. For some experiments, freshly isolated lysosome (1–5) and mitochondrial (8–12) fractions were treated with 200 μM GPN or 1% TritonX100 for 5 min at 4 °C (to minimize ATP degradation) to lyse lysosomes or mitochondria. Samples containing same amount of protein were loaded for the ATP assay (75 μg protein/well).

For ATP uptake assays, 0.2 μl of 2 mM ATP was added to 100 μl of samples (containing 75 μg of total protein) for an initial ATP concentration of 2×10^{-6} M. Samples luminescence was read over time, and the luminescence decay indicated active ATP uptake. Sample buffer served as a blank, and the decay of intrinsic luminescence was measured as background. In some experiments, freshly isolated lysosomes from cells pretreated with the inhibitors described above for 30 min at 37 °C were assayed immediately assayed for ATP uptake in the presence of those inhibitors. At the end of the assay, 0.1% TritonX100 was added to each sample to measure the total ATP released from vesicles.

Cell Viability Assay—Briefly, cells were transfected with the indicated DNA using Lipofectamine 2000 or electroporation. Cells were pretreated overnight with the inhibitors described above. Cells were stained with propidium iodide (Sigma, P-4170) (10 μg/ml) and incubated at room temperature in PBS for 15 min. Cells were then examined immediately by fluorescence microscopy (emission at 615 nm and excitation at 488 nm). For quantitative analysis, adherent cells were collected by trypsinization, and PI^+ and GFP^+ cells and GFP^+/PI^+ cells were counted using a hemocytometer under an upright fluorescent microscope.

For some assays, lactate dehydrogenase activity was determined by measuring NADH oxidation with pyruvate as substrate. For each assay, a 50-μl sample was incubated with 50 μl of reaction buffer (CytoTox-ONE™ homogeneous membrane integrity assay, Promega) for 10 min at 22 °C, and the fluorescence at 340 nm was measured using a spectrophotometer. Results were scaled to the complete cell death induced by exposure to 1% Triton X-100 at room temperature for 20 min. The percent of cell death was defined as 100 × (sample optical density− medium optical density)/(Triton X-100 optical density− medium optical density).

Data Analysis—Data are presented as mean ± S.E. Statistical comparisons were made using analysis of variance and Student's *t* test. $p < 0.05$ was considered to be statistically significant.

RESULTS

Inhibition of ATP Transport across the Lysosome Membrane by DIDS and Evans Blue—To directly measure ATP transport across the lysosomal membrane, we isolated lysosomes from HEK cells using density gradient centrifugation and assayed ATP uptake. We monitored ATP transport by evaluating ATP concentrations in the buffer using a bioluminescent ATP assay (9). A decrease of ATP concentration in the buffer suggested

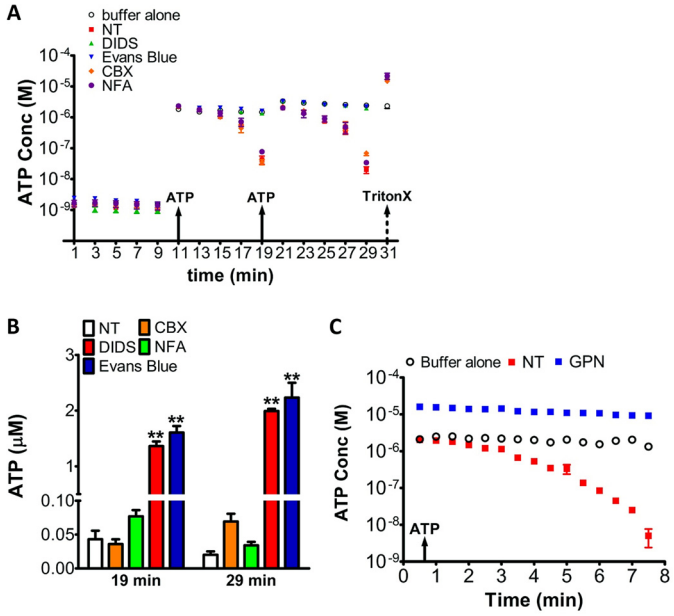

FIGURE 1. **ATP transport across lysosomal membrane is blocked by DIDS or Evans blue.** *A*, ATP uptake in isolated lysosomes is blocked by DIDS or Evans blue but not by CBX or NFA. Lysosomes isolated from HEK293T cells were treated with CBX, NFA, DIDS, or Evans blue (20 μM) for 30 min and then subjected to ATP uptake assays. Lysosomes were suspended in sodium-free homogenizing buffer (0.25 M sucrose, 1 mM EDTA, 10 mM HEPES (pH 7.0)) which was used under the "buffer alone" condition to detect intrinsic decay of ATP luminescence after ATP addition. At 11 and 21 min, ATP was added to 100 μl of sample to a final concentration (*Conc*) of 2 μM. Decay of ATP luminescence was detected over time as an indicator of active ATP uptake. At the end of the assay, 0.1% Triton X-100 was added to measure total ATP released from vesicles. *B*, ATP levels at 19 and 29 min. DIDS or Evans blue blocked ATP transport into lysosomes and resulted in higher extralysosome ATP levels relative to controls, whereas CBX or NFA treatment had no significant effect. Data were obtained from three independent experiments. *NT*, no treatment. **, $p < 0.01$. *C*, luminescence decay was observed in intact lysosomes but not in GPN (200 μM)-treated lysosomes, which release lysosomal ATP, or in buffer alone.

ATP uptake by lysosomes. We compared the luminescence decay over time following the repeated addition of ATP (2 μM) to lysosomes. As shown in Fig. 1*A*, control samples not treated with inhibitors showed ATP decrease rates of 12.26 ± 0.07%/min after the first ATP addition (11–19 min). Interestingly, that rate slowed to 5.00 ± 0.46%/min when lysosomes were pretreated with DIDS (20 μM) or Evans blue (20 μM), two known inhibitors of mammalian VNUT (3), for 30 min, and ATP was added in the presence of the inhibitors. In contrast, treatment of samples with CBX (20 μM) or NFA (20 μM), two inhibitors targeting both connexin and pannexin channels (11), had no effect.

For comparison, buffer ATP concentration 19 min after the first ATP application and 29 min after the second were replotted in Fig. 1*B*. Treatment with DIDS or Evans blue but not CBX or NFA significantly reduced ATP uptake. Buffers of DIDS and Evans blue-treated groups contained 1.36 ± 0.08 μM and 1.61 ± 0.12 μM ATP, respectively, at the 19-min time point after the first ATP addition, whereas the buffer of the non-treated group contained only 0.04 ± 0.01 μM ATP in the buffer (Fig. 1*B*). Consistent with the data from HEK cells, we also detected inhibition of ATP transport by DIDS, but not CBX, in lysosomes prepared from C2C12 cells (Fig. 4, *E–G*). Taken together, these

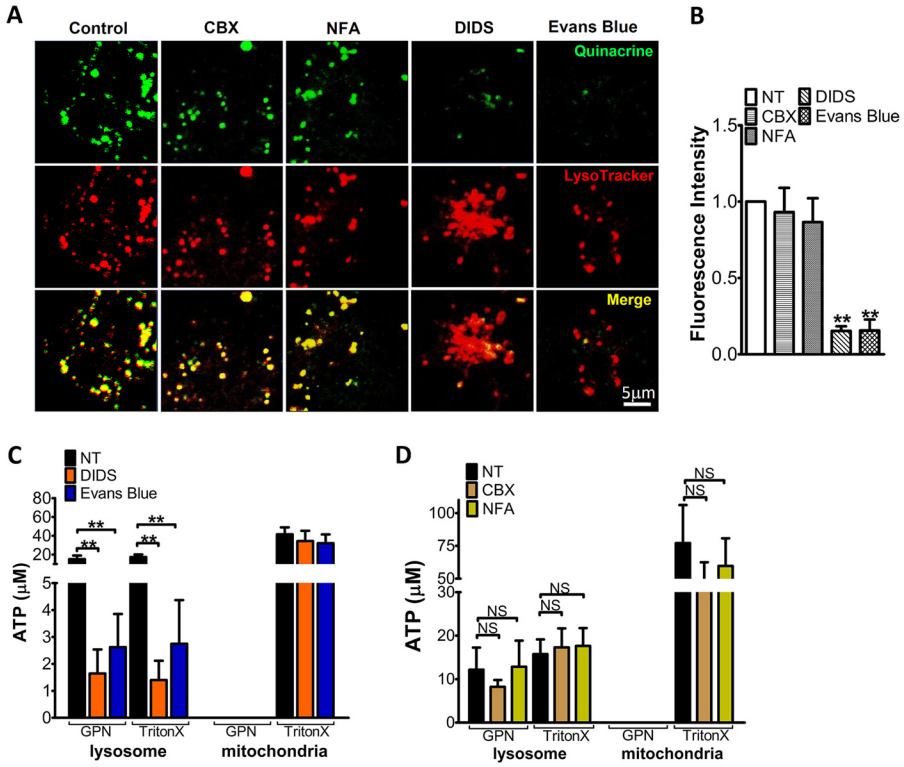

FIGURE 2. **DIDS and Evans Blue inhibit ATP accumulation in lysosomes.** *A*, COS1 cells were treated with inhibitors (CBX, 20 μM; NFA, 20 μM; DIDS, 20 μM; Evans blue, 20 μM) for 3 h at 37 °C, labeled with LysoTracker, and stained with quinacrine (10 μM). *B*, quinacrine fluorescence intensity of the images in *A*. Values were normalized to the fluorescence intensity of non-treated control cells. DIDS and Evans blue treatment dramatically decreased quinacrine intensity. The experiment was repeated three times. **, $p < 0.01$. C and *D*, DIDS and Evans blue, but not CBX and NFA, decreased lysosomal ATP accumulation. COS1 cells were treated with inhibitors at 20 μM for 3 h, and then cells were fractionated. Isolated lysosomal and mitochondrial fractions were collected and assayed for ATP content. Equal amount of samples on the basis of protein content (75 μg) were loaded per assay. GPN (200 μM) was used to lyse lysosomes. Data were obtained from three independent experiments. *NT*, no treatment; *NS*, no significance. **, $p < 0.01$.

data suggest the presence of a VNUT-like transporter in the lysosomes.

Loss of luminescence could be caused by ATP breakdown. To exclude this possibility, isolated lysosomes were treated with GPN (200 μM), a substrate of the lysosomal exopeptidase cathepsin C. GPN induces lysosome osmodialysis (6) and promotes the release of lysosomal ATP. After the addition of 2 μM ATP, we observed no significant luminescence decay in the GPN-treated group or the buffer control group. In contrast, non-treated lysosomes showed a dramatic loss of luminescence (Fig. 1*C*), suggesting that decreased luminescence was due to ATP uptake by lysosomes rather than ATP hydrolysis.

Inhibition of Lysosomal ATP Accumulation by DIDS and Evans Blue—If ATP accumulation is mediated by an ATP transporter, blocking that transporter should antagonize ATP deposition in lysosomes. To test this hypothesis, COS1 cells were treated with DIDS, Evans blue, CBX, or NFA, and ATP deposition was evaluated by the accumulation of quinacrine, a fluorescent dye used to locate intracellular ATP stores (6, 7, 12). As shown in Fig. 2*A*, quinacrine-labeled COS1 cells displayed a punctate granular pattern consistent with a vesicular origin, and puncta colocalized with LysoTracker and Lamp1staining (Fig. 5*A*), suggesting ATP accumulation in lysosomes. DIDS (20 μM) or Evans blue (20 μM) treatment significantly decreased quinacrine fluorescence (Fig. 2, *A* and *B*) by 84.71 ± 3.01 and 84.45 ± 7.25%, respectively. By contrast, treatment with CBX (20 μM) or NFA (20 μM) had no effect.

Lysosomal ATP levels were further measured by a bioluminescence assay using purified lysosomes from COS1 cells. High ATP concentrations in lysosome fractions, which were positive for the lysosome marker Lamp1, and in mitochondrial fractions, which were positive for the mitochondrial marker complex II, were detectable only after 5 min of treatment with 1% Triton X-100, indicating that ATP was contained within membrane-enclosed compartments (Fig. 2, *C* and *D*). Treatment of GPN (200 μM for 30 min) selectively increased the ATP levels in the lysosomal fractions but not mitochondrial fractions, suggesting a high lysosomal ATP concentration. Lysosomal ATP content (defined by the concentration of ATP released following GPN treatment) decreased remarkably from 15.15 ± 3.9 μM to 1.64 ± 0.89 μM or 2.62 ± 1.23 μM following treatment with DIDS or Evans blue, respectively (Fig. 2*C*), whereas CBX or NFA treatment (Fig. 2*D*) had no effect on comparable samples. Taken together, these data suggest that a VNUT-like transporter may mediate lysosomal ATP accumulation. They also suggest that DIDS and Evans blue slowly penetrate the cell membrane, although the mechanism remains unclear.

SLC17A9 Localization in Lysosomes—SLC17A9 reportedly localizes in secretory vesicles/granules (3–5). Our pharmacology data obtained using isolated lysosomes suggest that lysosomal membranes contain substantial amounts of SLC17A9 protein. To confirm this observation, lysosomal fractions of COS1 cells or COS1 cells expressing mSLC17A9-GFP (mouse SLC17A9-GFP) were enriched using density gradient centrifu-

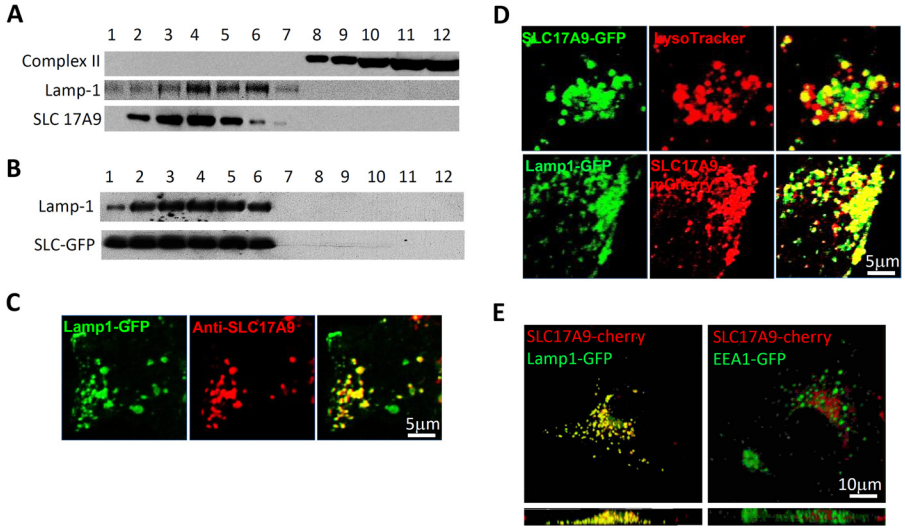

FIGURE 3. **SLC17A9 localizes to lysosomes.** *A*, detection of endogenous SLC17A9 in lysosomal fractions in COS1 cell. Bands of the predicted size of SLC17A9 were detected in Lamp1-positive fractions but not complex II-positive fractions. *B*, detection of overexpressed mSLC17A9-GFP in COS1 cell lysosomal fractions. *C*, endogenous SLC17A9 is located in Lamp1-GFP-expressing vesicles. Cells were transiently transfected with Lamp1-GFP, and endogenous SLC17A9 was detected by fluorescent staining. Note that a large amount of SLC17A9 protein is localized in Lamp1-positive puncta. *D*, overexpressed SLC17A9 is located primarily in LysoTracker- or Lamp1-GFP-positive organelles. The experiment was repeated three times, and representative images are shown. *E*, orthographic projection and side view of z-stack images to show lysosomal localization of SLC17A9.

gation, lysed, and then incubated with anti-SLC17A9 antibody. As shown in Fig. 3, *A* and *B*, both endogenous SLC17A9 and mSLC17A9-GFP were distributed to the Lamp1-positive fraction.

To further assess SLC17A9 subcellular localization, COS1 cells were transfected with Lamp1-GFP and then assessed with an SLC17A9 antibody. A large proportion of SLC17A9-positive puncta were also Lamp1-GFP-positive (Fig. 3*C*), suggesting that endogenous SLC17A9 is enriched in lysosomes. To evaluate the localization of exogenous SLC17A9, COS1 cells were transfected with mSLC17A9-GFP and labeled with LysoTracker or cotransfected with mSLC17A9-mCherry and Lamp1-GFP. Confocal imaging indicated a large proportion of exogenous mSLC17A9-GFP fluorescence in LysoTracker- or Lamp1-GFP-positive organelles (Fig. 3, *D* and *E*). Overall, our data suggest that both endogenous and heterologously expressed SLC17A9 is enriched in lysosomes.

SLC17A9 Mediates Lysosome ATP Transport—To test whether SLC17A9 is required for lysosomal ATP transport, C2C12 cells (a mouse cell line) were transfected with mSLC17A9-shRNA and then assayed for ATP transport. SLC17A9 expression levels in either C2C12 whole cell lysate (Fig. 4*A*) or lysosome lysate (Fig. 4*B*) from C2C12 culture were suppressed dramatically by mSLC17A9-shRNA expression. SLC17A9 silencing significantly decreased ATP transport in lysosomes isolated from C2C12 cells (Fig. 4, *C* and *D*). Although the initial ATP concentrations in buffer were comparable (~2 μM), by 21 min, ATP concentrations decreased to 0.14 ± 0.03 μM or 1.49 ± 0.23 μM in cells expressing scramble control shRNA or mSLC17A9-shRNA, respectively (Fig. 4*D*). Conversely, mSLC17A9-GFP overexpression dramatically increased lysosomal ATP uptake (Fig. 4, *E* and *F*). ATP concentrations in the buffer decreased to 0.023 ± 0.001 μM and 0.010 ± 0.001 μM in WT cells and cells expressing mSLC17A9-GFP, respectively, by 19 min after the first ATP addition, although initial ATP levels were comparable (~2.0 μM) (Fig. 4, *E* and *F*). As in WT cells, DIDS treatment inhibited ATP transport in cells expressing mSLC17A9-GFP. However, in mSLC17A9-GFP-expressing cells, a higher concentration (20 μM) of DIDS was required to suppress ATP transport to the same level as 5 μM DIDS did in WT cells. In contrast, 20 μM CBX (Fig. 4, *G* and *H*) did not inhibit ATP transport. Our data suggest that SLC17A9 is both sufficient and required for ATP transport across lysosomal membranes.

SLC17A9 Mediates Lysosome ATP Accumulation—To investigate SLC17A9 function in lysosomal ATP accumulation, quinacrine fluorescence was compared in C2C12 cells expressing Lamp1-mCherry or mSLC17A9-mCherry with or without mSLC17A9-shRNA. Robust quinacrine staining was observed in cells expressing Lamp1-mCherry, in cells expressing mSLC17A9-mCherry, and in cells expressing scrambled control shRNA and Lamp1-mCherry. However, cells expressing mSLC17A9-shRNA displayed little quinacrine staining (Fig. 5*A*). Relative to controls, the quinacrine intensity increased by 65.8% in SLC17A9-overexpressing cells but decreased by 84.2% in mSLC17A9-shRNA-overexpresseing cells (Fig. 5*B*).

Although quinacrine is commonly used as an ATP indicator (6, 7, 12), it has also been suggested to function as a pH indicator (13). Identification of SLC17A9 as a lysosome ATP transporter allowed us to clarify this. As shown in Fig. 5*C*, SLC17A9-deficient lysosomes showed strong LysoTracker staining, suggestive of an acidic pH, despite decreased lysosomal ATP content (Fig. 5*E*) and a decrease in quinacrine staining (Fig. 5*A*). These data suggest that quinacrine is likely an indicator of lysosome ATP but may not be a reliable indicator of pH. This is also in agreement with data showing decreased quinacrine staining but strong LysoTracker staining in DIDS-treated cells (Fig. 2*A*).

Lysosomal ATP accumulation was further evaluated by measuring ATP content in lysosomes purified from C2C12

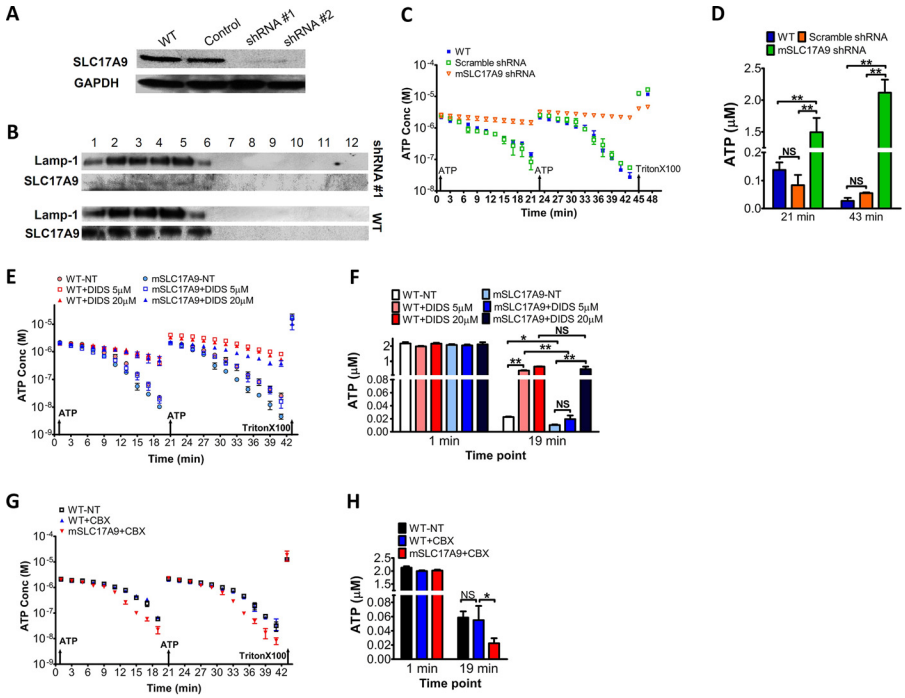

FIGURE 4. **ATP is transported into lysosomes through SLC17A9.** *A*, detection of mSLC17A9 in WT or mSLC17A9 knockdown C2C12 cells. Whole cell lysates were used, and GAPDH levels served as loading controls. *B*, detection of endogenous mSLC17A9 in isolated lysosomes of WT and mSLC17A9 knockdown C2C12 cells showing that endogenous protein levels are robustly down-regulated in the latter. *C*, SLC17A9 knockdown impairs lysosomal ATP uptake. Lysosomes of WT and mSLC17A9 knockdown C2C12 cells were isolated and assayed for ATP uptake. *Conc*, concentration. *A* and *D*, ATP levels at 21 and 43 min. The mSLC17A9-shRNA group showed significantly higher levels of ATP at 21 and 43 min, suggestive of impaired ATP transport. **, $p < 0.01$; *NS*, no significance. *E* and *F*, mSLC17A9-GFP overexpression facilitated ATP transport across lysosome membranes. 19 min after ATP addition, lysosomes from cells overexpressing mSLC17A9-GFP showed significant lower ATP levels than the WT group. DIDS (5 μM) significantly blocked ATP uptake in the WT group but not in the mSLC17A9-GFP-overexpressing group. DIDS (20 μM) blocked ATP uptake in both WT and mSLC17A9-GFP-overexpressing groups. *, $p < 0.05$; **, $p < 0.01$. *G* and *H*, CBX (20 μM) did not suppress ATP uptake mediated by mSLC17A9-GFP. The experiment was repeated three times in triplicate. *, $p < 0.05$.

cells. As shown in Fig. 5, *D* and *E*, mSLC17A9-GFP overexpression did not significantly increase GPN-induced ATP release from purified lysosomes. This outcome might be due to contamination of lysosomes isolated from non-transfected cells. However, mSLC17A9-shRNA dramatically decreased lysosomal ATP by 80.6% (from 12.04 ± 1.68 μM to 2.38 ± 0.49 μM). In contrast, ATP content in mitochondria was unchanged. Taken together, our data suggest that suppression of SLC17A9 significantly decreases lysosomal ATP accumulation, whereas its up-regulation has an opposing effect.

SLC17A9-mediated Lysosome ATP Accumulation Is Blocked by DIDS and Evans Blue—To further assess the role for SLC17A9 in lysosomal ATP accumulation, COS1 cells expressing mSLC17A9-mCherry were treated with inhibitors and then stained with quinacrine. As shown in Fig. 6, *A* and *B*, although DIDS (5 μM) or Evans blue (5 μM) treatment significantly decreased quinacrine intensity in WT cells by 84.64 ± 6.39% or 84.32 ± 10.39%, respectively, those treatments had little effect on quinacrine intensity in mSLC17A9-mCherry-expressing cells. However, a higher concentration of DIDS (20 μM) or Evans blue (20 μM) was sufficient to eliminate quinacrine staining in mSLC17A9-mCherry-expressing cells (Fig. 6, *A* and *B*). In contrast, CBX treatment did not decrease quinacrine intensity in wild-type or mSLC17A9-mCherry-expressing cells. Accordingly, DIDS (5 μM) or Evans blue (5 μM) treatment significantly decreased ATP content (from 20.67 ± 2.96 μM to 1.60 ± 0.70 μM or 0.88 ± 0.14 μM, respectively) in lysosomes purified from WT cells. However, higher (20 μM) concentrations of DIDS or Evans blue were required to significantly decrease ATP contents in lysosomes isolated from mSLC17A9-mCherry-expressing cells (Fig. 6*C*). Lysosomal ATP content in cells expressing mSLC17A9-mCherry were decreased by 86.29 ± 5.40% (from 24.67 ± 1.45 μM to 3.27 ± 1.27 μM) or by 92.73 ± 3.19% (to 1.70 ± 0.67 μM), respectively, when DIDS (20 μM) or Evans blue (20 μM) was applied. These data suggest that SLC17A9 overexpression increases ATP transport efficiency, and, hence, higher levels of DIDS and Evans blue are required to inhibit ATP accumulation. These data are also in accordance with findings from the ATP uptake assay (Fig. 4, *E* and *F*). Overall, lysosomal SLC17A9 expression is sufficient to accumulate ATP, an activity blocked by DIDS or Evans blue.

SLC17A9 Deficiency Promotes Cell Death—C2C12 cells expressing mSLC17A9-shRNA appeared rounder, suggesting that SLC17A9 loss compromises cell survival. To assess this possibility, we monitored cell death in C2C12 cells using propidium iodide (PI) staining. In cells expressing control scramble shRNA, PI staining was observed in 4.11 ± 0.99% of attached cells. In contrast, 38.44 ± 5.63% of attached cells expressing mSLC17A9-shRNA were PI positive (Fig. 7, *A* and *B*). In agreement with this, DIDS (5 μM or 20 μM) treatment, but not CBX or NFA treatment, dramatically increased PI-positive cells in COS1 cells (Fig. 7, *C* and *D*). PI-positive attached cells were increased from 3.31 ± 1.28% in control to 33.00 ± 5.86% (5 μM

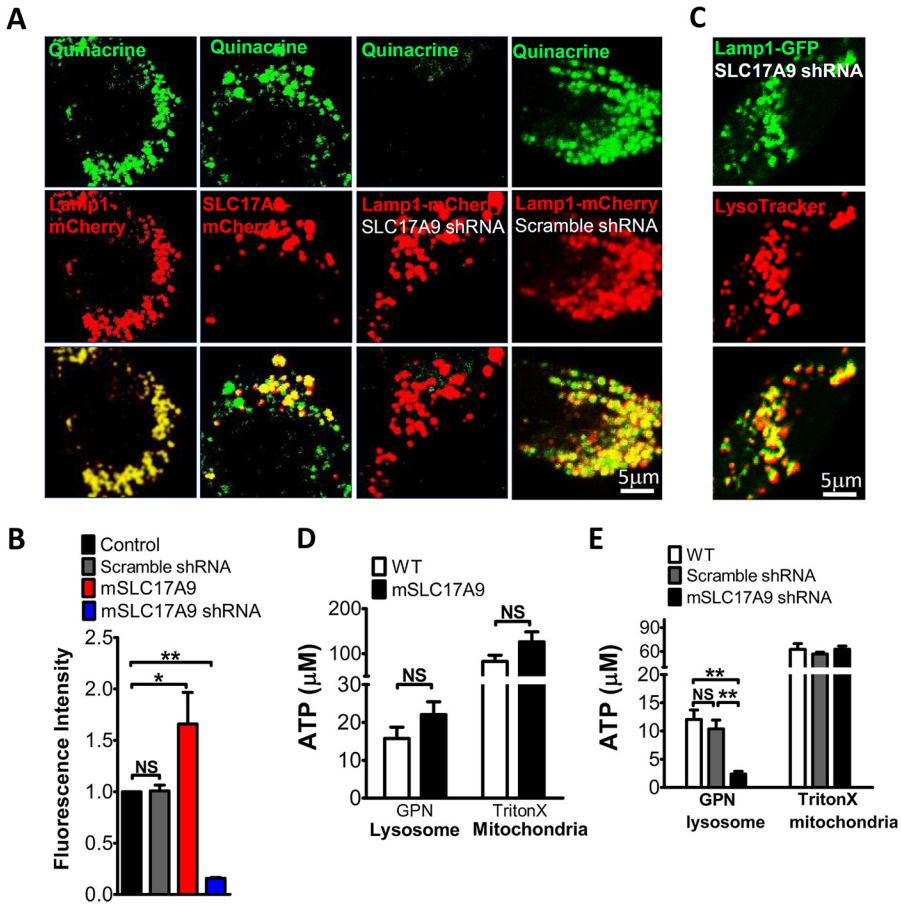

FIGURE 5. **SLC17A9 mediates lysosomal ATP accumulation.** *A* and *B*, mSLC17A9 overexpression increases lysosomal ATP accumulation, whereas mSLC17A9 knockdown has the opposite effect. Lysosomal ATP levels were monitored using quinacrine (10 μM) staining. Lamp1-mCherry served as a lysosome marker. Values were normalized to non-treated control cells. The experiment was repeated three times, and representative images are shown. *, $p < 0.05$; **, $p < 0.01$; *NS*, no significance. *C*, SLC17A9 knockdown has no effect on LysoTracker staining. *D*, mSLC17A9-GFP overexpression does not alter lysosomal ATP content, possibly because of contamination of lysosomes isolated from non-transfected cells. *E*, reduced ATP content in lysosomes of mSLC17A9 knockdown C2C12 cells. The experiment was repeated three times in triplicate. **, $p < 0.01$.

DIDS) and 76.00 ± 4.58% (20 μM DIDS) in DIDS-treated groups. Given that 5 μM DIDS inhibited lysosomal ATP accumulation in WT cells but not mSLC17A9-GFP-expressing cells, overexpression may rescue the cell death phenotypes observed in cells treated with 5 μM DIDS. As shown in Fig. 7, *C* and *D*, the number of PI-positive attached COS1 cells decreased to 8.67 ± 1.76% when mSLC17A9-GFP, but not Lamp1-GFP (data not shown), was overexpressed. Such rescue was not observed in mSLC17A9-GFP-expressing cells treated with 20 μM DIDS, a finding in agreement with the observation that 20 μM DIDS inhibited lysosomal ATP accumulation in COS1 cells expressing mSLC17A9-GFP (Fig. 6). We also assessed cell death associated with SLC17A9 loss by assaying the levels of lactate dehydrogenase, a cytosolic enzyme that is released into cell culture medium when cells lose membrane integrity. Both DIDS (5 μM or 20 μM) treatment and SLC17A9 knockdown dramatically increased cell death on the basis of the lactate dehydrogenase assay. Specifically, DIDS treatment induced 55.58 ± 3.07% (5 μM) and 68.13 ± 3.34% (20 μM) cell death, whereas SLC17A9 silencing induced 39.95 ± 8.00% cell death in C2C12 cells (Fig. 7*E*).

SLC17A9 Suppression Promotes Lysosomal Dysfunction—To confirm that SLC17A9 knockdown promotes lysosomal dysfunction potentially associated with cell death, we assessed lysosomal function using DQ-BSA, a dye that indicates active proteolysis in lysosomes. Strong DQ-BSA signals were seen in control C2C12 cells, as anticipated, but not in cells expressing mSLC17A9-shRNA (Fig. 8*A*), suggesting that mSLC17A9 loss compromises lysosomal function. In agreement, treatment of C2C12 cells with DIDS (at 5 and 20 μM) but not CBX (20 μM) reduced DQ-BSA staining (Fig. 8*B*). mSLC17A9-GFP overexpression rescued attenuated DQ-BSA staining induced by 5 μM but not 20 μM DIDS, suggesting that lysosome dysfunction induced by 5 μM DIDS results from SLC17A9 loss.

Dysfunction of lysosomes promotes accumulation of proteins, lipids, and carbohydrates, which may be further converted to a non-degradable oxidized polymeric substance called lipofuscin, also referred to as "aging pigment." Autofluorescence (green) detectable within the excitation wavelength of 480 nm is an indicator of lipofuscin accumulation (14). Although we observed no significant autofluorescence in control cells, mSLC17A9 knockdown cells showed strong autofluorescence (Fig. 8*C*), which was also observed after cells were treated with DIDS but not CBX (Fig. 8*D*). Taken together, our data suggest that lysosomal SLC17A9 is critical for lysosomal function and that lysosomal SLC17A9 might underlie cell death.

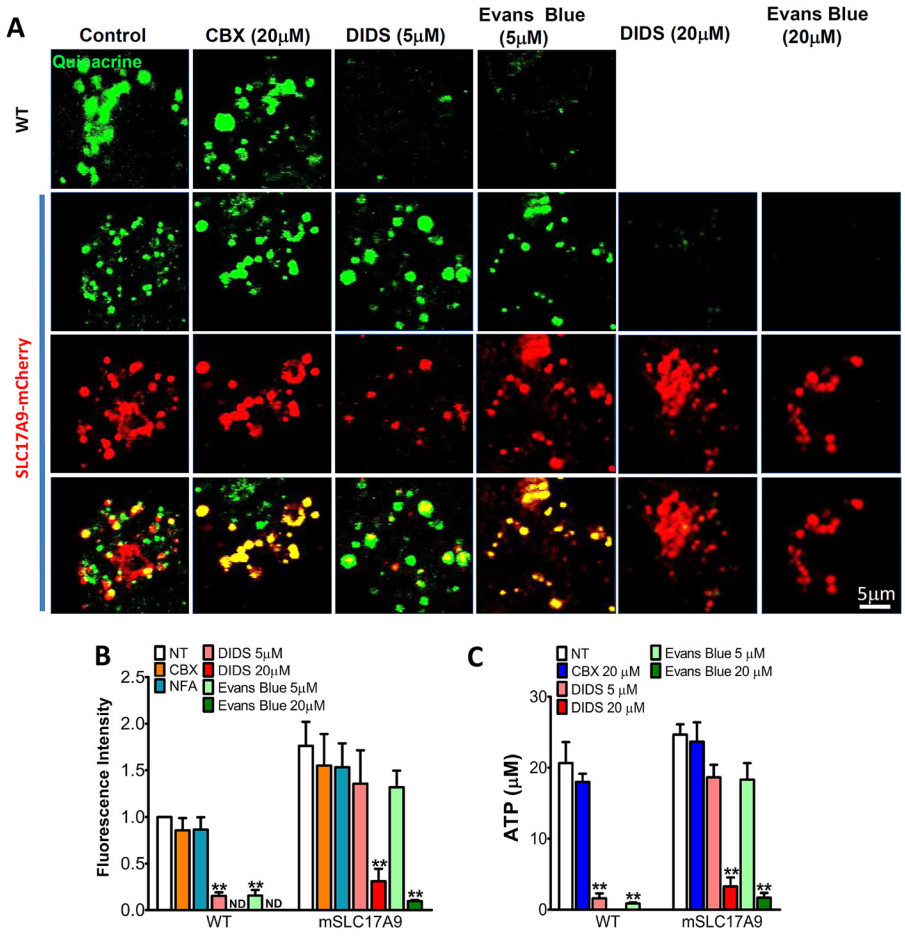

FIGURE 6. **DIDS and Evans blue blocked the ATP transport activity of overexpressed SLC17A9.** *A*, higher (20 μM) concentrations of DIDS and Evans blue are required to block ATP accumulation in lysosomes expressing mSLC17A9-GFP. Quinacrine fluorescence served to monitor ATP levels in lysosomes. WT COS1 cells and cells transiently overexpressing mSLC17A9-mCherry were treated with CBX (20 μM), 5 μM or 20 μM DIDS, or Evans blue. At 5 μM, DIDS or Evans blue treatment significantly reduced ATP content in lysosomes in WT COS1 cells but not in mSLC17A9-mCherry overexpressing cells. DIDS and Evans blue at 20 μM had a dramatic effect in reducing ATP accumulation in lysosomes of mSLC17A9-mCherry-expressing COS1 cells. CBX treatment did not have a significant effect on lysosomal ATP levels. *B*, quinacrine fluorescence intensity of the images in *A*. **, $p < 0.01$; *ND*, non-detectable. *C*, measurement of ATP levels in lysosomes isolated from WT or SLC17A9-overexpressing COS1 cells with or without pretreatment with inhibitors. Higher concentrations of DIDS and Evans blue were required to suppress ATP accumulation in lysosomes of mSLC17A9-mCherry-expressing COS1 cells. GPN was used to release lysosomal ATP. The experiment was repeated three times in triplicate. **, $p < 0.01$.

DISCUSSION

Previous studies have indicated that ATP is enriched in lysosomes of astrocytes and microglia cells and is released through lysosomal exocytosis in response to various stimuli (6, 7). We have also reported that lysosomes in COS1, HEK293, and C2C12 cells contain high (~millimolar) ATP levels (12). However, the mechanisms underlying ATP accumulation in those organelles remained unclear. Emerging evidence suggests that VNUT (also called SLC17A9) could be a lysosomal ATP transporter (15), but controversy remains (16). In particular, evidence supporting a lysosomal localization of endogenous SLC17A9 or lysosomal ATP transport activity via SLC17A9 was lacking. Here, using quinacrine staining, a bioluminescent ATP assay, and ATP uptake assays, we provide strong evidence that SLC17A9 is responsible for lysosomal ATP accumulation.

Previously, vesicular neurotransmitter transporters (vesicular glutamate transporters and VNUT/SLC17A9) have been shown to take up glutamate or ATP into synaptic vesicles or secretory vesicles using membrane potential driven by V-ATPase (3, 17–19). Like synaptic vesicles and secretory vesicles, V-ATPase in the lysosome membranes generates substantial voltage potential and an H^+ gradient (20, 21). Therefore, is likely that SLC17A9 transports ATP into lysosomes using the membrane potential established by V-ATPase, although confirmation of this awaits further investigation.

Although DIDS is often used as a SLC17A9 blocker (3, 17), it also reportedly blocks other transporters (22). Here, however, we propose that defects in ATP uptake and accumulation induced by DIDS were primarily due to SLC17A9 inhibition. We conclude this for the following reasons. We showed that DIDS directly inhibited SLC17A9-mediated ATP uptake in isolated lysosomes, we observed a correlation between SLC17A9 levels and DIDS concentrations required to inhibit ATP transport as well as ATP accumulation (Figs. 4 and 6), and effects on DIDS treatment were rescued by overexpression of SLC17A9-GFP (Figs. 7*C* and 8*B*).

Quinacrine has been used as an indicator of lysosomal pH (13). However, quinacrine also binds ATP with a high affinity (23, 24) and is commonly used to visualize ATP-containing vesicles, including lysosomes (6, 7, 25, 26). We provide new evi-

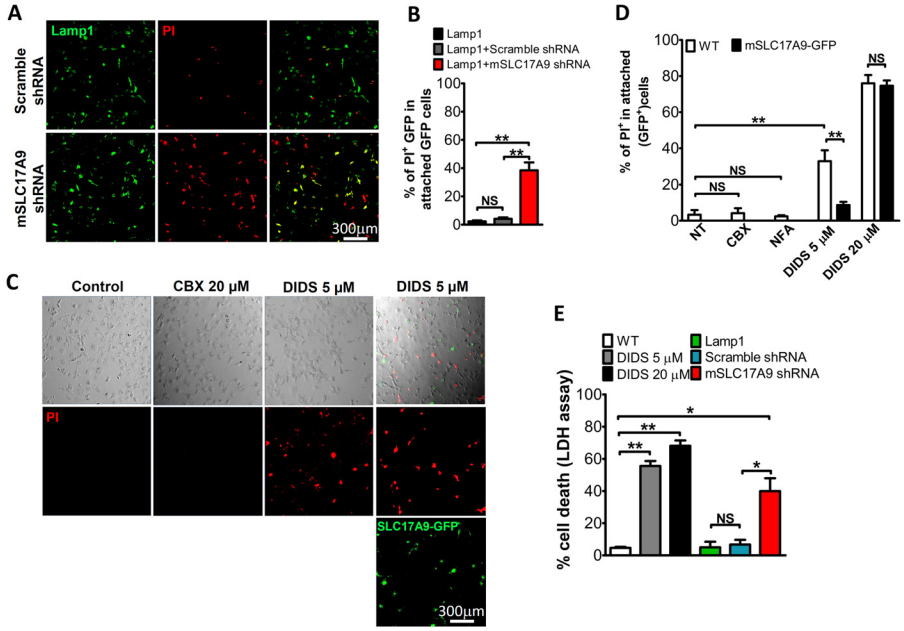

FIGURE 7. **Suppression of SLC17A9 is associated with cell death.** *A*, PI staining of C2C12 cells overexpressing Lamp1-GFP or Lamp1-GFP and mSLC17A9-shRNA. SLC17A9 knockdown significantly increased the percentage of PI-positive cells. *B*, percentage of PI^+ adherent GFP^+ cells from *A*. **, $p < 0.01$; *NS*, not significant. *C* and *D*, DIDS (5 or 20 μM) but not CBX (20 μM) treatment dramatically increased the percentage of PI^+ cells. COS1 cells were treated with CBX (20 μM) or DIDS (5 or 20 μM) for 24 h and stained with PI. The percentage of PI^+ cells induced by DIDS (5 μM) was decreased significantly when mSLC17A9-GFP was overexpressed. **, $p < 0.01$. *E*, the percentage of cell viability indicated by the lactate dehydrogenase assay in C2C12 cell culture supernatants increases following DIDS treatment or mSLC17A9 knockdown. Supernatants of knockdown cells or cells treated with either 5 or 20 μM of DIDS for 24 h were collected and assayed for lactate dehydrogenase activity. A positive control defining 100% cell death was created by treating cells with 5% Triton X-100 for 20 min at room temperature. The experiment was repeated three times in triplicate. *, $p < 0.05$; **, $p < 0.01$.

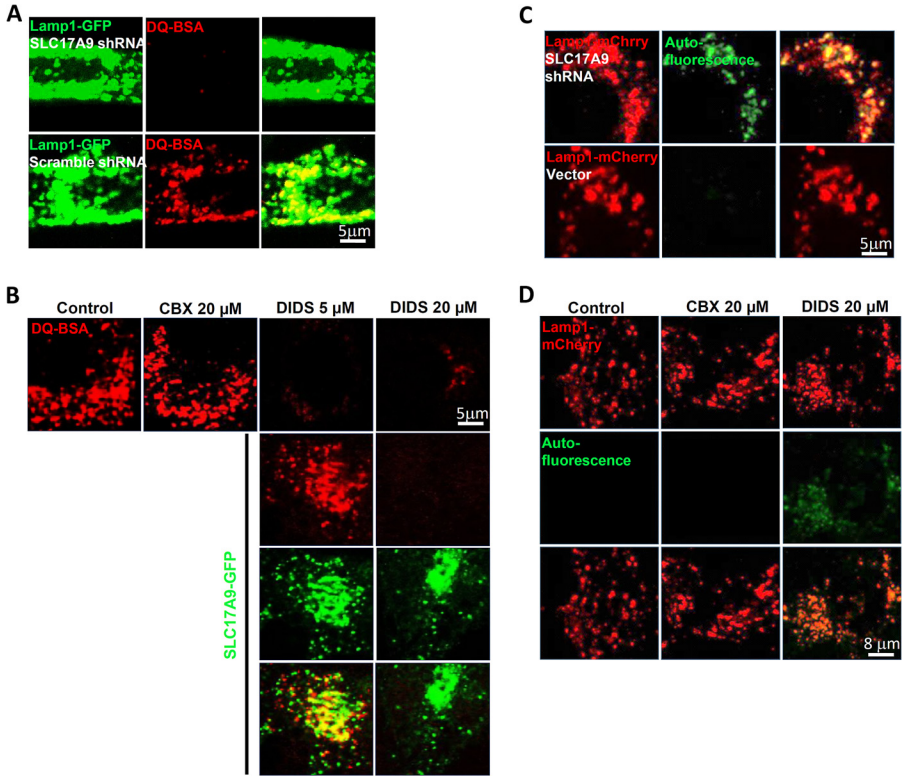

FIGURE 8. **SLC17A9 inhibition promotes lysosomal dysfunction.** *A*, decreased DQ-BSA fluorescence in lysosomes of C2C12 mSLC17A9 knockdown cells. C2C12 cells were transfected with Lamp1-GFP plus SLC17A9-shRNA or Lamp1-GFP plus scrambled shRNA control. 24 h after transfection, cells were loaded with DQ-BSA and analyzed by confocal microscopy. *B*, treatment with DIDS but not CBX reduces DQ-BSA fluorescence. WT cells treated with DIDS or CBX for 24 h and loaded with DQ-BSA. DIDS at 5 μM but not 20 μM induced loss of DQ-BSA staining, an effect rescued by SLC17A9 overexpression. *C*, C2C12 cells were transfected with Lamp1-GFP plus SLC17A9-shRNA or Lamp1-GFP plus pSUPER vector. Lysosomal autofluorescence was observed in mSLC17A9 knockdown cells but not in control Lamp1-GFP cells. Autofluorescence was detected at an excitation wavelength of 480 nm. *D*, DIDS-treated cells showed lysosomal autofluorescence, but non-treated and CBX-treated cells did not. Cells were transfected with Lamp1-Cherry to label lysosomes and treated with either CBX (20 μM) or DIDS (20 μM) for 8 h. The experiment was repeated three times, and representative images are shown.

dence that quinacrine intensity correlates with lysosomal ATP levels rather than lysosomal acidic pH. Several lines of evidence support this. Although quinacrine staining was altered by both suppression (Figs. 2*A* and 5*A*) or overexpression (Fig. 5*A*) of SLC17A9, lysosomal pH, as indicated by LysoTracker staining, remained unchanged in either case (Figs. 2*A*, 3*D*, and 5*C*). SLC17A9 knockdown eliminated quinacrine staining in lysosomes (Fig. 5). Quinacrine intensity was correlated with lysosomal ATP content, as measured using the ATP bioluminescent assay in all experiments. Therefore, our data suggest that quinacrine is an indicator for ATP content in acidic compartments.

SLC17A9 reportedly functions in insulin secretion through vesicular ATP release in β cells (5), in exocytosis of ATP-enriched vesicles in biliary epithelial cells (25), and in exocytosis of ATP-enriched vesicles during T cell activation (4). However, the identities of the ATP-containing vesicles in these studies are unclear. We showed that SLC17A9 is highly enriched in lysosomes in several cell types, including C2C12, COS1, and HEK293T cells (Fig. 1 and data not shown), although a portion of SLC17A9 is distributed in non-lysosomal vesicles. Therefore, in these cells, lysosomes may be the major secretory vesicles that release ATP. Previously, others have reported that ATP accumulated in lysosomes of astrocytes (6, 26) and microglia (7) and lysosomal ATP release via lysosomal exocytosis is implicated in ischemic insult (6) and cell migration (7). However, the molecular mechanisms underlying ATP accumulation in these cells remain elusive. On the basis of the data presented here, SLC17A9 might be an important lysosomal ATP transporter in astrocytes and microglia cells as well and potentially function in microglia migration and ischemic damage.

The cell types used in this study exhibit little lysosomal exocytosis. This raises the question of why these cells need to store ATP in lysosomes. Lysosomes contain hydrolases that degrade organelles and macromolecules delivered to the lysosomal compartment by autophagy, endocytosis, or phagocytosis. Lysosomal dysfunction causes lysosomal storage and lipofuscin accumulation and, subsequently, leads to cell death (27). We showed that cells with compromised SLC17A9 lacked DQ-BSA staining and accumulated lipofuscin in lysosomes, suggesting defective lysosome function. Likewise, inhibition of SLC17A9-mediated ATP transport into lysosomes was correlated with significant cell death, although the mechanism underlying that outcome remains unknown. ATP reportedly activates proteases such as cathepsin D and increase proteolysis within lysosomes (28), and cathepsin D deficiency induced lysosomal storage of lipofuscin (29). Our data suggest that SLC17A9 regulates lysosomal proteolysis by maintaining ATP at levels sufficient to activate proteases, such as cathepsin D, within the compartment. Therefore, compromised SLC17A9 function could attenuate cathepsin D activity and promote subsequent lipofuscin accumulation and cell death.

In summary, we present the first direct evidence that that SLC17A9 actively transports ATP across the lysosomal membrane in several cell types. Compromised SLC17A9 leads to reduced ATP accumulation in lysosomes and dysfunctional lysosomes and, subsequently, to cell death. Therefore, ATP functions not only as cellular energy currency but is also critical for lysosome function.

Acknowledgments—We thank Haoxing Xu for assistance and support. We also thank other members of the Dong laboratory for encouragement and comments.

REFERENCES

1. Hediger, M. A., Clémençon, B., Burrier, R. E., and Bruford, E. A. (2013) The ABCs of membrane transporters in health and disease (SLC series): introduction. *Mol. Aspects Med.* **34,** 95–107
2. Fredriksson, R., Nordström, K. J., Stephansson, O., Hägglund, M. G., and Schiöth, H. B. (2008) The solute carrier (SLC) complement of the human genome: phylogenetic classification reveals four major families. *FEBS Lett.* **582,** 3811–3816
3. Sawada, K., Echigo, N., Juge, N., Miyaji, T., Otsuka, M., Omote, H., Yamamoto, A., and Moriyama, Y. (2008) Identification of a vesicular nucleotide transporter. *Proc. Natl. Acad. Sci. U.S.A.* **105,** 5683–5686
4. Tokunaga, A., Tsukimoto, M., Harada, H., Moriyama, Y., and Kojima, S. (2010) Involvement of SLC17A9-dependent vesicular exocytosis in the mechanism of ATP release during T cell activation. *J. Biol. Chem.* **285,** 17406–17416
5. Geisler, J. C., Corbin, K. L., Li, Q., Feranchak, A. P., Nunemaker, C. S., and Li, C. (2013) Vesicular nucleotide transporter-mediated ATP release regulates insulin secretion. *Endocrinology* **154,** 675–684
6. Zhang, Z., Chen, G., Zhou, W., Song, A., Xu, T., Luo, Q., Wang, W., Gu, X. S., and Duan, S. (2007) Regulated ATP release from astrocytes through lysosome exocytosis. *Nat. Cell Biol.* **9,** 945–953
7. Dou, Y., Wu, H. J., Li, H. Q., Qin, S., Wang, Y. E., Li, J., Lou, H. F., Chen, Z., Li, X. M., Luo, Q. M., and Duan, S. (2012) Microglial migration mediated by ATP-induced ATP release from lysosomes. *Cell Res.* **22,** 1022–1033
8. Corriden, R., and Insel, P. A. (2010) Basal release of ATP: an autocrine-paracrine mechanism for cell regulation. *Sci. Signal.* **3,** re1
9. Haanes, K. A., and Novak, I. (2010) ATP storage and uptake by isolated pancreatic zymogen granules. *Biochem. J.* **429,** 303–311
10. Suadicani, S. O., Brosnan, C. F., and Scemes, E. (2006) P2X7 receptors mediate ATP release and amplification of astrocytic intercellular Ca^{2+} signaling. *J. Neurosci.* **26,** 1378–1385
11. Harris, A., and Locke, D. (2009) Pannexins or connexins? in *Connexins: a guide* (Dahl, G., and Harris, A. L., eds), pp. P287–P301, Humana Press, Clifton, NJ
12. Huang, P., Zou, Y., Zhong, X. Z., Cao, Q., Zhao, K., Zhu, M. X., Murrell-Lagnado, R., and Dong, X. P. (2014) P2X4 forms functional ATP-activated cation channels on lysosomal membranes regulated by luminal pH. *J. Biol. Chem.* **289,** 17658–17667
13. Lee, C. (1971) A fluorescent probe of the hydrogen ion concentration in ethylenediaminetetraacetic acid particles of beef heart mitochondria. *Biochemistry* **10,** 4375–4381
14. Dong, X. P., Cheng, X., Mills, E., Delling, M., Wang, F., Kurz, T., and Xu, H. (2008) The type IV mucolipidosis-associated protein TRPML1 is an endolysosomal iron release channel. *Nature* **455,** 992–996
15. Oya, M., Kitaguchi, T., Yanagihara, Y., Numano, R., Kakeyama, M., Ikematsu, K., and Tsuboi, T. (2013) Vesicular nucleotide transporter is involved in ATP storage of secretory lysosomes in astrocytes. *Biochem. Biophys. Res. Commun.* **438,** 145–151
16. Imura, Y., Morizawa, Y., Komatsu, R., Shibata, K., Shinozaki, Y., Kasai, H., Moriishi, K., Moriyama, Y., and Koizumi, S. (2013) Microglia release ATP by exocytosis. *Glia* **61,** 1320–1330
17. Miyaji, T., Sawada, K., Omote, H., and Moriyama, Y. (2011) Divalent cation transport by vesicular nucleotide transporter. *J. Biol. Chem.* **286,** 42881–42887
18. Omote, H., Miyaji, T., Juge, N., and Moriyama, Y. (2011) Vesicular neurotransmitter transporter: bioenergetics and regulation of glutamate transport. *Biochemistry* **50,** 5558–5565
19. El Mestikawy, S., Wallén-Mackenzie, A., Fortin, G. M., Descarries, L., and

Trudeau, L. E. (2011) From glutamate co-release to vesicular synergy: vesicular glutamate transporters. *Nat. Rev. Neurosci.* **12,** 204–216
20. Koivusalo, M., Steinberg, B. E., Mason, D., and Grinstein, S. (2011) *In situ* measurement of the electrical potential across the lysosomal membrane using FRET. *Traffic* **12,** 972–982
21. Cheng, X., Shen, D., Samie, M., and Xu, H. (2010) Mucolipins: Intracellular TRPML1–3 channels. *FEBS Lett.* **584,** 2013–2021
22. Omote, H., and Moriyama, Y. (2013) Vesicular neurotransmitter transporters: an approach for studying transporters with purified proteins. *Physiology* **28,** 39–50
23. Irvin, J. L., and Irvin, E. M. (1954) The interaction of quinacrine with adenine nucleotides. *J. Biol. Chem.* **210,** 45–56
24. White, P. N., Thorne, P. R., Housley, G. D., Mockett, B., Billett, T. E., and Burnstock, G. (1995) Quinacrine staining of marginal cells in the stria vascularis of the guinea-pig cochlea: a possible source of extracellular ATP? *Hear. Res.* **90,** 97–105
25. Sathe, M. N., Woo, K., Kresge, C., Bugde, A., Luby-Phelps, K., Lewis, M. A., and Feranchak, A. P. (2011) Regulation of purinergic signaling in biliary epithelial cells by exocytosis of SLC17A9-dependent ATP-enriched vesicles. *J. Biol. Chem.* **286,** 25363–25376
26. Liu, T., Sun, L., Xiong, Y., Shang, S., Guo, N., Teng, S., Wang, Y., Liu, B., Wang, C., Wang, L., Zheng, L., Zhang, C. X., Han, W., and Zhou, Z. (2011) Calcium triggers exocytosis from two types of organelles in a single astrocyte. *J. Neurosci.* **31,** 10593–10601
27. Aits, S., and Jäättelä, M. (2013) Lysosomal cell death at a glance. *J. Cell Sci.* **126,** 1905–1912
28. Pillai, S., and Zull, J. E. (1985) Effects of ATP, vanadate, and molybdate on cathepsin D-catalyzed proteolysis. *J. Biol. Chem.* **260,** 8384–8389
29. Koike, M., Nakanishi, H., Saftig, P., Ezaki, J., Isahara, K., Ohsawa, Y., Schulz-Schaeffer, W., Watanabe, T., Waguri, S., Kametaka, S., Shibata, M., Yamamoto, K., Kominami, E., Peters, C., von Figura, K., and Uchiyama, Y. (2000) Cathepsin D deficiency induces lysosomal storage with ceroid lipofuscin in mouse CNS neurons. *J. Neurosci.* **20,** 6898–6906
30. Wang, X., Zhang, X., Dong, X. P., Samie, M., Li, X., Cheng, X., Goschka, A., Shen, D., Zhou, Y., Harlow, J., Zhu, M. X., Clapham, D. E., Ren, D., and Xu, H. (2012) TPC proteins are phosphoinositide-activated sodium-selective ion channels in endosomes and lysosomes. *Cell* **151,** 372–383
31. Dong, X. P., Shen, D., Wang, X., Dawson, T., Li, X., Zhang, Q., Cheng, X., Zhang, Y., Weisman, L. S., Delling, M., and Xu, H. (2010) PI(3,5)P(2) controls membrane trafficking by direct activation of mucolipin Ca(2+) release channels in the endolysosome. *Nat. Commun.* **1,** 38